# Results of Phosphorus Magnetic Resonance Spectroscopy for Brain Metastases Correlate with Histopathologic Results

*Johannes Kerschbaumer[1], Daniel Pinggera[1], Ruth Steiger[2], Andreas Rietzler[2], Adelheid Wöhrer[4], Marina Riedmann[3], Astrid Ellen Grams[2], Claudius Thomé[1], Christian Franz Freyschlag[1]*

■ BACKGROUND: **Brain metastases (BMs) are classically well-circumscribed lesions. Still, the amount of edema in these neoplasms suggests either mechanisms of infiltration or defense. A better understanding of the mechanisms within the edema of BMs seems reasonable to preoperatively identify areas of potential infiltration and resect them. BMs represent tumors with high energy demand and cell turnover; therefore, they qualify for preoperative investigation with phosphorus-31 magnetic resonance spectroscopy (31PMRS), which reveals information about those characteristics.**

■ METHODS: **Ten patients with BMs were included in this trial. All underwent preoperative standard magnetic resonance imaging with additional 31PMRS. In all patients, 1 voxel within the contrast-enhancing tumor (CE+), 1 voxel at the border (including CE+ areas and surrounding T2-hyperintensive [T2+] areas), and 1 distant voxel purely including T2+ areas were determined by a neuroradiologist and a neurosurgeon. A frameless stereotactic biopsy was performed after craniotomy. Subsequently, the metabolites of the 31PMRS were analyzed and compared with the histopathologic results.**

■ RESULTS: **Ratios, reflecting resynthesis (CE+/border/T2+: 1.109 ± 0.192/1.112 ± 0.158/1.083 ± 0.097), hydrolysis (0.303 ± 0.089/0.360 ± 0.122/0.321 ± 0.089), energy demand (4.227 ± 2.35/3.453 ± 1.284/3.599 ± 0.833), and membrane turnover (1.239 ± 0.2611/3.453 ± 1.284/3.599 ± 0.283) were calculated and compared intraindividually with a voxel from the contralateral side (resynthesis/hydrolysis/energy demand/membrane turnover: 1.063 ± 0.085/0.335 ± 0.073/3.317 ± 0.7573/0.784 ± 0.186), respectively. Resynthesis showed a trend toward higher ratios in CE+ and border biopsies without reaching statistical significances. This trend was also seen concerning energy demand. Membrane turnover was significantly higher in CE+, border zone, and also in the T2+ areas compared with controls (*P* > 0.001).**

■ CONCLUSIONS: **31PMRS in BMs provides information on metabolic changes in tumor and surrounding edema. There is proof of enhanced metabolism in tissue without histologic tumor manifestation.**

## INTRODUCTION

Brain metastases (BMs) are typically well-circumscribed lesions that differ from glioma and in which tumor cells are known to migrate along white matter tracts. The formation of perilesional edema surrounding BMs still suggests either mechanisms of infiltration or a reaction of defense. Recent studies have demonstrated that BMs are able to infiltrate the surrounding brain,[1,2] suggesting that patients would benefit from supramarginal resection, even if direct tumor manifestation within the surrounding edema has not been proven.[3,4] The discovery of immunomodulatory agents (e.g., programmed death ligand 1, cytotoxic T-lymphocyte-associated protein 4) has revealed that

**Key words**
- 31-P-MRS
- Biopsy
- Brain metastases
- Infiltration
- Spectroscopy

**Abbreviations and Acronyms**
**31PMRS**: Phosphorus-31 magnetic resonance spectroscopy
**ATP**: Adenosine triphosphate
**BM**: Brain metastasis
**CE+**: Contrast-enhancing tumor
**PCr**: Phosphocreatine
**Pi**: Free phosphate
**T2+**: T2-hyperintensive

*From the Departments of [1]Neurosurgery, [2]Neuroradiology, and [3]Medical Statistics, Informatics and Health Economics, Medical University of Innsbruck, Innsbruck; and [4]Institute of Neurology, Medical University Vienna, Vienna, Austria*

*To whom correspondence should be addressed: Johannes Kerschbaumer, M.D. [E-mail: johannes.kerschbaumer@tirol-kliniken.at]*

*Citation: World Neurosurg. (2019) 127:e172-e178.*
*https://doi.org/10.1016/j.wneu.2019.03.041*

*Journal homepage: **www.journals.elsevier.com/world-neurosurgery***

*Available online: **www.sciencedirect.com***

**Table 1.** Patient Characteristics

| Characteristics | Value |
|---|---|
| Age (years) | |
| Mean ± standard error of mean | 60.5 ± 11 |
| Range | 41–75 |
| Sex | |
| Female | 4 |
| Male | 6 |
| Primary tumor | |
| NSCLC | 6 |
| Malignant melanoma | 2 |
| Breast cancer | 1 |
| Gastrointestinal cancer | 1 |
| Systemic disease at the time of surgery | |
| First diagnosis | 4 |
| Stable | 3 |
| Progressive | 3 |
| Preoperative Karnofsky Performance Status Scale score | |
| Mean ± standard error of mean | 95 ± 6 |
| Range | 80–100 |
| Preoperative need of steroids (mg) | |
| Mean ± standard error of mean | 8.6 ± 4.2 |
| Range | 0–12 |
| Hemisphere | |
| Right | 6 |
| Left | 4 |
| Lobe | |
| Frontal | 4 |
| Parietal | 2 |
| Occipital | 3 |
| Temporal | 1 |
| Duration of surgery (minutes) | |
| Mean ± standard error of mean | 178.5 ± 45 |
| Range | 90–240 |
| Duration of biopsies (minutes) | |
| Mean ± standard error of mean | 18.9 ± 4 |
| Range | 10–25 |

Values are number of patients or as otherwise indicated.
NSCLC, non-small cell lung cancer.

inflammatory processes at the brain/metastasis interface have prognostic[5] and therapeutic implications,[6] especially in stage IV melanomas and non-small cell lung cancers that have metastasized to the central nervous system.[7] Currently, many investigators focus on performing histopathologic examinations for the presence or absence of infiltration to serve as a prognostic factor. This aims at preoperatively identifying patients at high risk of intracranial recurrence, and consequently performing more aggressive resections. To achieve this goal, it is imperative to change the classic surgical approach to BMs from a circumferential preparation along the pseudocapsule toward a supramarginal resection including the infiltrative zone adjacent to the tumor.

The criterion standard for detection of BMs is magnetic resonance imaging, but areas of cellular infiltration are missed with standard morphologic imaging protocols. Modern magnetic resonance imaging algorithms may enhance discovery of areas at high risk by adding perfusion imaging, spectroscopy, and diffusion-weighted imaging.[8] BMs are shown to have a high energy demand and cell turnover; therefore, they qualify for a preoperative investigation with phosphorus-31 magnetic resonance spectroscopy (31PMRS). It is our goal to reveal information about these malignant characteristics[9–12] within areas adjacent to the contrast-enhancing tumor using these advance magnetic resonance imaging sequences. With a better understanding of the mechanisms involved in infiltration and edema around BMs, we hope to identify areas of potential infiltration preoperatively.

## METHODS

### Study Design

This trial represents a cohort study of a selected patient cohort with BMs, amiable for supramarginal resection.

### Setting

Ten consecutive patients, presenting to our department with a BM, scheduled for microsurgical resection, were included in this trial over a period of 12 months.

### Participants

Patients who fulfilled the criteria for surgical resection of BMs in a noneloquent location amenable for supramarginal resection were included in this trial. They had to be able to understand and sign a written informed consent form and agree to undergo an advanced magnetic resonance investigation, including 31PMRS. Histopathologic confirmation of a BM and an early postoperative magnetic resonance imaging were mandatory.

A total of 10 patients (Table 1) were included in this prospective trial after providing informed consent. In addition to 31PMRS, all patients underwent structural magnetic resonance imaging examination of the brain, according to a standardized tumor protocol, which contains T2-and T1-weighted contrast-enhanced sequences, such as pre- and postcontrast 3-dimensional magnetization-prepared rapid gradient-echo T1-weighted sequence, diffusion-weighted and perfusion-weighted imaging sequence, coronal T2-weighted fluid-attenuated inversion recovery, and axial 2-dimensional T2-weighted turbo spin-echo.

### Variables

***Imaging.*** 31PMRS was performed with a 3-T whole-body system (Verio [Siemens Medical AG, Erlangen, Germany]) with a double-tuned proton/phosphorus volume head coil (Rapid Biomedical,

Würzburg, Germany). For each patient, one magnetic resonance spectroscopy 3-dimensional block, based on a previously acquired T2 space sequence, of the whole brain was recorded. The volume of interest was obtained with an extrapolated $8 \times 8 \times 16$ matrix and a field of view of $240 \times 240$ mm$^2$, resulting in a voxel size of $15 \times 15 \times 25$ mm$^3$.

31PMRS data were processed offline with the jMRUI software package (version 5.0, available at http://www.mrui.uab.es), using the nonlinear least square fitting algorithm AMARES.[13] Phosphocreatine (PCr), adenosine triphosphate (ATP), free phosphate (Pi), and the phospho-mono-esther and phospho-di-esther could be determined from the single voxels of interest. Because of interindividual differences in the spectra, ratios representing resynthesis (PCr/ATP), hydrolysis (Pi/ATP), energy demand (PCr/Pi), and membrane turnover (phospho-mono-esther/phosphor-di-esther) were calculated and compared with a voxel from the contralateral healthy side of the same individual (predefined voxel from the frontal white matter). Subsequently, the metabolites of the 31PMRS (including contralateral control) were analyzed and compared with the histopathologic results.

### Planning and Execution of Surgery

In each patient, 1 voxel within the contrast-enhancing tumor (CE+), 1 voxel at the border (including CE+ areas and surrounding T2-hyperintensive [T2+] areas), and 1 distant voxel, purely including T2+ areas (but amenable for supramarginal resection), were determined by a neuroradiologist and a neurosurgeon. A frameless stereotactic biopsy was performed after craniotomy prior to the opening of the dura to avoid brain shift and guarantee the accuracy of the specimen. One biopsy from the tumor itself (CE+), 1 at the border of CE+ area to the surrounding edema, and 1 distant biopsy (T2+) within the edema but without contrast-enhancing signal were harvested. The specimens were immediately fixed in formalin and prepared for further neuropathologic analysis.

Subsequently, the metabolites of 31PMRS (including contralateral control) were analyzed in correlation to the histopathologic results.

After completion of the biopsies, standard image-guided resection of the metastasis was performed. Use of intraoperative fluorescence and sonography were at the surgeon's discretion.

### Statistical Analysis

Continuous variables are reported as mean ± standard error of mean; nominal variables are reported as frequencies and ratios. The calculated ratios were tested for normality using the Shapiro-Wilk test for normality. If the variables were distributed normally, a t test was performed to check for significant differences. For nonnormal distributed values, nonparametric tests were performed. $P < 0.05$ was considered statistically significant.

## RESULTS

### Participants

We prospectively included 10 patients with assumed BM of different primary tumors in this study. All patients fulfilled the criteria for surgical resection because of mass effect of the tumor. Except for 1 patient, who was asymptomatic, all were pretreated with steroids for 3 ± 3 days before the surgical intervention, with a mean dose of 8.6 mg/d (range, 0–12 mg) (Table 1).

### Surgery

The extra time to take the 3 biopsies accounted for 19 minutes of additional duration of surgery (range, 10–25 minutes), with a mean total operating room time for resection of 179 minutes (range, 90–240 minutes).

### Histopathologic Results

Histopathologic diagnosis confirmed BM in all cases, with a predominance for non-small cell lung cancer (Table 1).

**CE+.** There was obvious evidence of tumor manifestation in all biopsies (10/10) taken from the CE+ areas.

***Border.*** There were 2 biopsies from the border zone without clear tumor manifestation and 1 case where signs of reactive gliosis and cell irregularities were present, but without distinct tumor cells.

**T2+.** Two biopsies with unambiguous tumor cell manifestations (2/10) within the cohort of biopsies taken from T2+ areas were found. The remaining biopsies of the T2+ areas showed no tumor cells.

### 31PMRS

Resynthesis, displayed as the ratio of PCr/ATP, showed a trend toward higher rates in CE+ and border biopsies without reaching statistical significance. This trend was also seen for energy demand, with the highest ratios within the CE+ voxel, but failed to reach statistical significance. Membrane turnover was significantly higher in CE+, border, and T2+ compared with control ($P < 0.001$) (Figure 1). Furthermore, there was no difference in the membrane turnover between the metastasis itself (CE+) and the surrounding edema (T2+) ($P = 0.645$).

Comparing the voxels containing tumor cells proven by histopathologic examination with the voxels where no tumor cells were found, there was no statistically significant difference in the ratios for resynthesis ($P = 0.497$), hydrolysis ($P = 0.859$), energy demand ($P = 0.866$), or membrane turnover ($P = 0.340$) (Figure 2).

## DISCUSSION

In our study, several parameters of energy metabolism were assessed with 31PMRS in and around BM. One distinct goal of this study was to determine pathogenicity of perilesional edema and to gather proof of perilesional infiltration.

The origin of the voluminous perilesional edema in BM remains unclear. Several theories have been postulated, from a pure vasogenic fluid collection because of the BM's mass effect to a more active mechanism. It is unclear whether this active mechanism is either a bystander effect of immunologic defense from glia cells or attributable to the invasive patterns of the BM. The amount of edema surrounding BM has also been assessed as a predictor of outcome in BM with conflicting results.[14,15] The edema itself does not seem to be an independent risk factor for recurrence, but it has been hypothesized that it might correlate with a more invasive growth pattern.

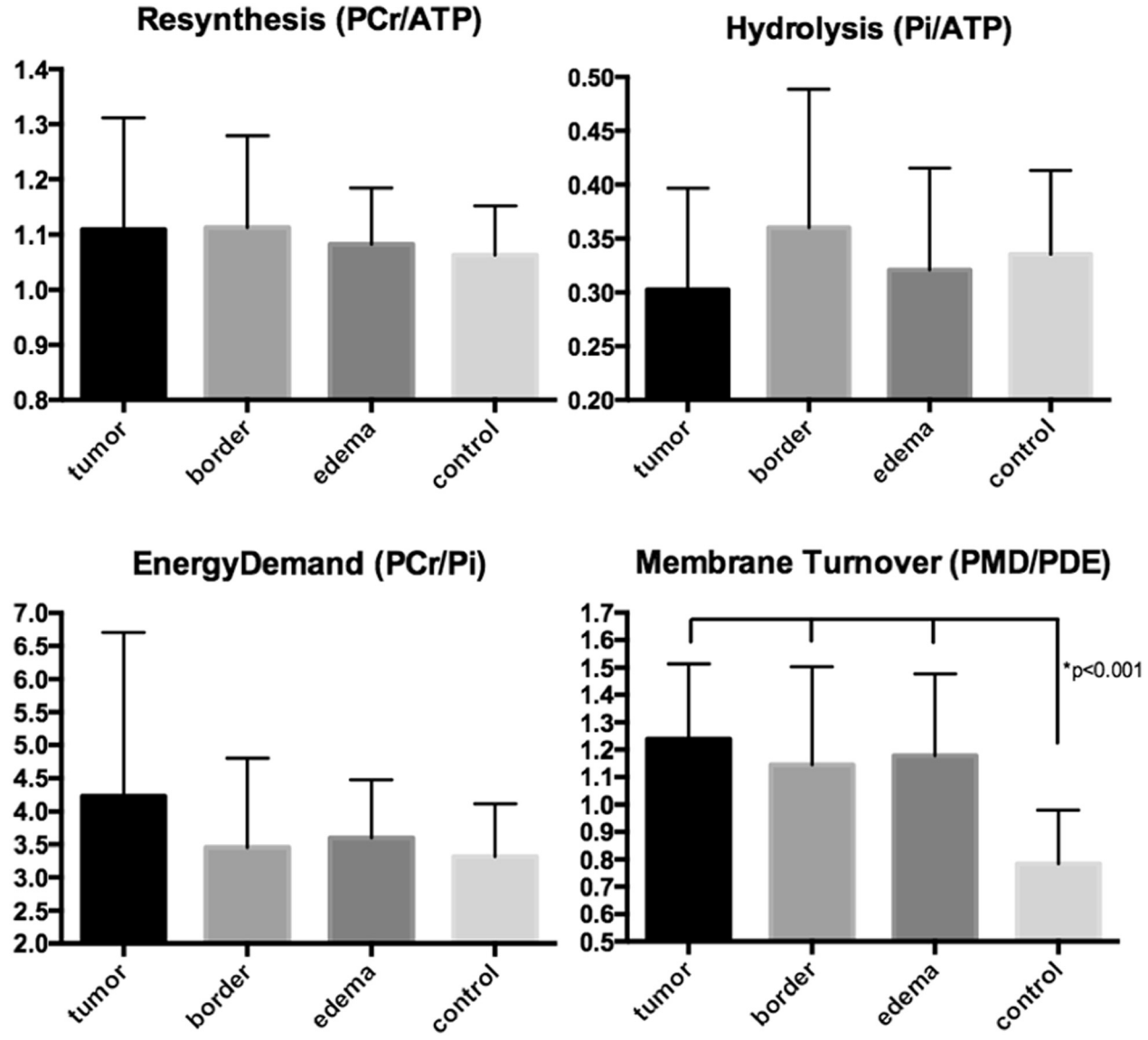


| | CE+ | BORDER | T2+ | control | p-value |
|---|---|---|---|---|---|
| Resynthesis | 1.109±0.192 | 1.112±0.158 | 1.083±0.097 | 1.063±0.085 | 0.520 |
| Hydrolysis | 0.303±0.089 | 0.360±0.122 | 0.321±0.089 | 0.335±0.073 | 0.406 |
| Energy demand | 4.227±2.35 | 3.453±1.284 | 3.599±0.833 | 3.317±0.7573 | 0.880 |
| Membrane turnover | 1.239±0.2611 | 3.453±1.284 | 3.599±0.283 | 0.784±0.186 | *<0.001* |

**Figure 1.** Ratios of phosphorus-31 magnetic resonance spectroscopy metabolites in relation to classical morphologic magnetic resonance imaging regions determined by contrast uptake and T2 changes. Values for resynthesis, hydrolysis, energy demand, and membrane turnover are shown (means ± SDs). ATP, adenosine triphosphate; CE+, contrast-enhancing tumor; PCr, phosphocreatine; PDE, phosphor-di-esther; Pi, free phosphate; PMD, phospho-mono-esther; T2+, T2-hyperintensive.

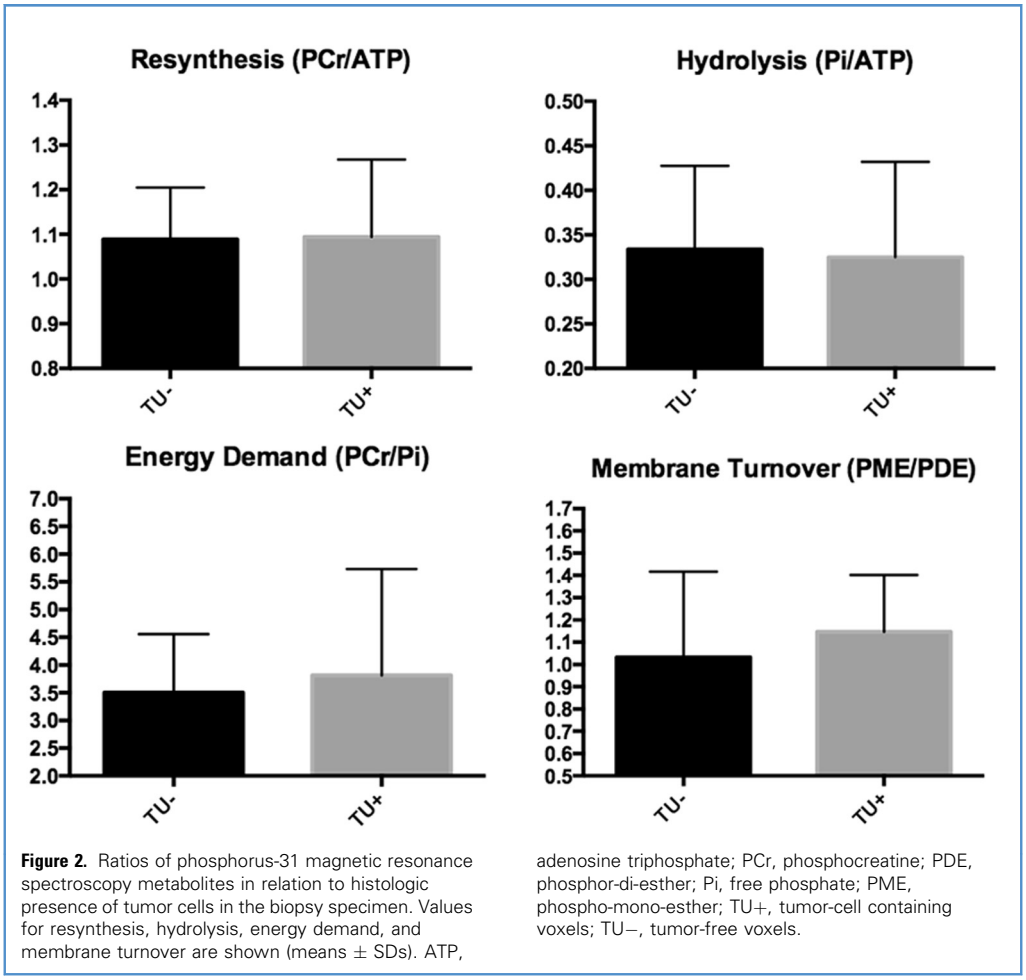


**Figure 2.** Ratios of phosphorus-31 magnetic resonance spectroscopy metabolites in relation to histologic presence of tumor cells in the biopsy specimen. Values for resynthesis, hydrolysis, energy demand, and membrane turnover are shown (means ± SDs). ATP, adenosine triphosphate; PCr, phosphocreatine; PDE, phosphor-di-esther; Pi, free phosphate; PME, phospho-mono-esther; TU+, tumor-cell containing voxels; TU−, tumor-free voxels.

Proton magnetic resonance spectroscopy was used mainly for differentiation between normal tissue, BM, or malignant glioma, on the basis that metabolites of cell damage around the CE+ lesions may be increased in glioma because of their more infiltrative nature compared with BM.

It has been proven that membrane biosynthesis is enhanced within the tumor.[16] The elevated membrane turnover of the peritumoral margin zone (T2+) could be explained by the voxel size because areas from the tumor itself may be included in the metabolic spectrum. Possibly, there were zones of CE+ tissue included in the analyzed volumes. The augmented metabolism in distant areas, with underlying tumor-free histopathology, represent a novel finding. Traditionally, surrounding areas of BMs show no contrast enhancement,[17] but we found a significantly enhanced metabolism because this was displayed by the ratio of membrane turnover. It may support the hypothesis on the inflammatory microenvironment surrounding metastases, where T cells and tumor-associated macrophages acted as antitumor immune response.[5,6] There are several steps known to be necessary for invasion of the brain and crossing the blood−brain barrier.[18,19] Cells adapt and interact with the local microenvironment for survival. Previously, Paget[20] described the formation of BM by the seed and soil theory. The essential part of metastasis formation remains within the target tissue.[21,22] Additionally, it has been shown that several tumor cells remain in a dormant state, without developing clinical significance.[23]

The therapeutic armamentarium available to neurooncologists is limited to radiotherapy, radiosurgery, and surgical resection.[24-26] The efficacy of additional chemotherapy has not been proven.[27] Resection of BM without adjuvant radiotherapy has resulted in a local relapse up to 60% within 1 year.[28,29] By adding adjuvant whole-brain radiotherapy, 20%−30% of the patients recurred within 2 years after initial treatment.[29] Whole-brain radiotherapy after local treatment of BM becomes increasingly problematic with longer survival of the patients. The increasing evidence of neurocognitive deterioration[30,31] and poor quality of life[32] requires the need for alternative treatment options, especially because whole-brain radiotherapy has failed to increase overall survival in most randomized controlled trials.[29,30] This could indicate the presence of some dormant tumor cells within the surrounding peritumoral niche of BM that are unresponsive to radiation therapy. Possibly, this challenge in adjuvant treatment could be solved with a more aggressive surgical strategy. Microsurgical techniques have evolved dramatically within the past 15 years. Use of intraoperative monitoring,[4] image guidance,[3] and fluorescence-guided surgery[33-38] are widely available. Reliable

identification of the tumor extent, notwithstanding the disruption of the blood–brain barrier, is important for the estimation of resection probability, and necessary for supratotal resection of BM.

Our study has technical limitations, represented in the comparatively large size of the voxels in the 31PMRS. The method has flaws in detection within very small areas of infiltration. Furthermore, the small sample size is clearly a limitation that has to be mentioned.

Histologic proof of cancer invasion to the perilesional tissue and preoperative 31PMRS diagnosis may change the surgical perspective for the treatment of BM toward a more radical surgical approach. This requires further investigations because a better understanding of infiltrative mechanisms will increase the therapeutic potential for the future.

## CONCLUSIONS

31PMRS of BM provides information on metabolic changes in CE+ tumors and surrounding edema. The elevated membrane turnover may indicate the active defense mechanisms of glial cells that counteracted infiltrative attempts of tumor cells. There is a proof of enhanced metabolism in tissue without histologic tumor manifestation. The mechanisms leading to the usually overproportionate amount of edema remain unclear, requiring further research about this neuro-oncologic phenomenon.

## REFERENCES

1. Berghoff AS, Rajky O, Winkler F, et al. Invasion patterns in brain metastases of solid cancers. *Neuro Oncol*. 2013;15:1664-1672.
2. Siam L, Bleckmann A, Chaung HN, et al. The metastatic infiltration at the metastasis/brain parenchyma-interface is very heterogeneous and has a significant impact on survival in a prospective study. *Oncotarget*. 2015;6:29254-29267.
3. Yoo H, Kim YZ, Nam BH, et al. Reduced local recurrence of a single brain metastasis through microscopic total resection. *J Neurosurg*. 2009;110:730-736.
4. Kamp MA, Dibue M, Niemann L, et al. Proof of principle: supramarginal resection of cerebral metastases in eloquent brain areas. *Acta Neurochir (Wien)*. 2012;154:1981-1986.
5. Berghoff AS, Preusser M. The inflammatory microenvironment in brain metastases: potential treatment target? *Chin Clin Oncol*. 2015;4:21.
6. Berghoff AS, Ricken G, Wilhelm D, et al. Tumor infiltrating lymphocytes and PD-L1 expression in brain metastases of small cell lung cancer (SCLC). *J Neurooncol*. 2016;130:19-29.
7. Goldberg SB, Gettinger SN, Mahajan A, et al. Pembrolizumab for patients with melanoma or non-small-cell lung cancer and untreated brain metastases: early analysis of a non-randomised, open-label, phase 2 trial. *Lancet Oncol*. 2016;17:976-983.
8. Chiang IC, Kuo YT, Lu CY, et al. Distinction between high-grade gliomas and solitary metastases using peritumoral 3-T magnetic resonance spectroscopy, diffusion, and perfusion imagings. *Neuroradiology*. 2004;46:619-627.
9. Lehnhardt FG, Rohn G, Ernestus RI, Grune M, Hoehn M. 1H- and (31)P-MR spectroscopy of primary and recurrent human brain tumors in vitro: malignancy-characteristic profiles of water soluble and lipophilic spectral components. *NMR Biomed*. 2001;14:307-317.
10. Hattingen E, Jurcoane A, Bahr O, et al. Bevacizumab impairs oxidative energy metabolism and shows antitumoral effects in recurrent glioblastomas: a 31P/1H MRSI and quantitative magnetic resonance imaging study. *Neuro Oncol*. 2011;13:1349-1363.
11. Hattingen E, Lanfermann H, Menon S, et al. Combined 1H and 31P MR spectroscopic imaging: impaired energy metabolism in severe carotid stenosis and changes upon treatment. *MAGMA*. 2009;22:43-52.
12. Hattingen E, Magerkurth J, Pilatus U, Hubers A, Wahl M, Ziemann U. Combined (1)H and (31)P spectroscopy provides new insights into the pathobiochemistry of brain damage in multiple sclerosis. *NMR Biomed*. 2011;24:536-546.
13. Vanhamme L, van den Boogaart A, Van Huffel S. Improved method for accurate and efficient quantification of MRS data with use of prior knowledge. *J Magn Reson*. 1997;129:35-43.
14. Spanberger T, Berghoff AS, Dinhof C, et al. Extent of peritumoral brain edema correlates with prognosis, tumoral growth pattern, HIF1a expression and angiogenic activity in patients with single brain metastases. *Clin Exp Metastasis*. 2013;30:357-368.
15. Kerschbaumer J, Bauer M, Popovscaia M, Grams AE, Thome C, Freyschlag CF. Correlation of tumor and peritumoral edema volumes with survival in patients with cerebral metastases. *Anticancer Res*. 2017;37:871-875.
16. Ciminera AK, Jandial R, Termini J. Metabolic advantages and vulnerabilities in brain metastases. *Clin Exp Metastasis*. 2017;34:6-7.
17. Parizel PM, Degryse HR, Gheuens J, et al. Gadolinium-DOTA enhanced MR imaging of intracranial lesions. *J Comput Assist Tomogr*. 1989;13:378-385.
18. Eichler AF, Chung E, Kodack DP, Loeffler JS, Fukumura D, Jain RK. The biology of brain metastases-translation to new therapies. *Nat Rev Clin Oncol*. 2011;8:344-356.
19. Preusser M, Capper D, Ilhan-Mutlu A, et al. Brain metastases: pathobiology and emerging targeted therapies. *Acta Neuropathol*. 2012;123:205-222.
20. Paget S. The distribution of secondary growths in cancer of the breast. 1889. *Cancer Metastasis Rev*. 1989;8:98-101.
21. Sierra A, Price JE, Garcia-Ramirez M, Mendez O, Lopez L, Fabra A. Astrocyte-derived cytokines contribute to the metastatic brain specificity of breast cancer cells. *Lab Invest*. 1997;77:357-368.
22. Lin Q, Balasubramanian K, Fan D, et al. Reactive astrocytes protect melanoma cells from chemotherapy by sequestering intracellular calcium through gap junction communication channels. *Neoplasia*. 2010;12:748-754.
23. Vanharanta S, Massague J. Origins of metastatic traits. *Cancer Cell*. 2013;24:410-421.
24. Gaspar LE, Mehta MP, Patchell RA, et al. The role of whole brain radiation therapy in the management of newly diagnosed brain metastases: a systematic review and evidence-based clinical practice guideline. *J Neurooncol*. 2010;96:17-32.
25. Kalkanis SN, Kondziolka D, Gaspar LE, et al. The role of surgical resection in the management of newly diagnosed brain metastases: a systematic review and evidence-based clinical practice guideline. *J Neurooncol*. 2010;96:33-43.
26. Linskey ME, Andrews DW, Asher AL, et al. The role of stereotactic radiosurgery in the management of patients with newly diagnosed brain metastases: a systematic review and evidence-based clinical practice guideline. *J Neurooncol*. 2010;96:45-68.
27. Mehta MP, Paleologos NA, Mikkelsen T, et al. The role of chemotherapy in the management of newly diagnosed brain metastases: a systematic review and evidence-based clinical practice guideline. *J Neurooncol*. 2010;96:71-83.
28. Patchell RA, Tibbs PA, Regine WF, et al. Postoperative radiotherapy in the treatment of single metastases to the brain: a randomized trial. *JAMA*. 1998;280:1485-1489.
29. Kocher M, Soffietti R, Abacioglu U, et al. Adjuvant whole-brain radiotherapy versus observation after radiosurgery or surgical resection of one to three cerebral metastases: results of the EORTC 22952-26001 study. *J Clin Oncol*. 2011;29:134-141.
30. Brown PD, Jaeckle K, Ballman KV, et al. Effect of radiosurgery alone vs radiosurgery with whole brain radiation therapy on cognitive function in patients with 1 to 3 brain metastases: a randomized clinical trial. *JAMA*. 2016;316:401-409.
31. Chang EL, Wefel JS, Hess KR, et al. Neurocognition in patients with brain metastases treated with radiosurgery or radiosurgery plus whole-

brain irradiation: a randomised controlled trial. *Lancet Oncol*. 2009;10:1037-1044.

32. Soffietti R, Kocher M, Abacioglu UM, et al. A European Organisation for Research and Treatment of Cancer phase III trial of adjuvant whole-brain radiotherapy versus observation in patients with one to three brain metastases from solid tumors after surgical resection or radiosurgery: quality-of-life results. *J Clin Oncol*. 2013;31:65-72.

33. Hohne J, Hohenberger C, Proescholdt M, et al. Fluorescein sodium-guided resection of cerebral metastases-an update. *Acta Neurochir (Wien)*. 2017;159:363-367.

34. Schebesch KM, Brawanski A, Hohenberger C, Hohne J. Fluorescein sodium-guided surgery of malignant brain tumors: history, current concepts, and future project. *Turk Neurosurg*. 2016;26:185-194.

35. Schebesch KM, Hoehne J, Hohenberger C, et al. Fluorescein sodium-guided resection of cerebral metastases-experience with the first 30 patients. *Acta Neurochir (Wien)*. 2015;157:899-904.

36. Kamp MA, Fischer I, Buhner J, et al. 5-ALA fluorescence of cerebral metastases and its impact for the local-in-brain progression. *Oncotarget*. 2016;7:66776-66789.

37. Kamp MA, Grosser P, Felsberg J, et al. 5-aminolevulinic acid (5-ALA)-induced fluorescence in intracerebral metastases: a retrospective study. *Acta Neurochirur (Wien)*. 2012;154:223-228 [discussion: 228].

38. Widhalm G. Intra-operative visualization of brain tumors with 5-aminolevulinic acid-induced fluorescence. *Clin Neuropathol*. 2014;33:260-278.

*Conflict of interest statement: The authors declare that the article content was composed in the absence of any commercial or financial relationships that could be construed as a potential conflict of interest.*

*Received 4 February 2019; accepted 5 March 2019*

*Citation: World Neurosurg. (2019) 127:e172-e178.*
*https://doi.org/10.1016/j.wneu.2019.03.041*

*Journal homepage:* ***www.journals.elsevier.com/world-neurosurgery***

*Available online:* ***www.sciencedirect.com***